Synthesis of new dyes from imidazo[1,2-*a*]pyridine: tautomerism, spectroscopic characterisation, DFT/TD-DFT calculations, atoms in molecules analyses and antibacterial activities

Samaneh Mohammadi, Mehdi Pordel*, Sadegh Allameh and Hamed Chegini

Department of Chemistry, Mashhad Branch, Islamic Azad University, Mashhad, Iran

The synthesis, optical properties, theoretical calculations and antibacterial activity of a series of new heterocyclic dyes from imidazo[1,2-*a]* pyridine are described. The key intermediate 2-[3-(hydroxyimino)imidazo[1,2-*a*]pyridin-2(3*H*)-ylidene]malononitrile was obtained *via* the nucleophilic substitution of hydrogen in 3-nitroimidazo[1,2-*a*]pyridine with malononitrile in basic methanol solution. Tautomerism, oxidation and alkylation studies on the dye led to the synthesis of new heterocyclic indigo-coloured, purple, and orange dyes in good yields. The structures of all newly synthesised compounds were confirmed by spectral and analytical data. The optical properties of the dyes were spectrally characterised and shown to exhibit interesting photophysical properties including high extinction coefficients. Density functional theory calculations of the dyes were performed to provide the optimised geometries and relevant frontier orbitals. Calculated electronic absorption spectra were also obtained by the time-dependent density functional theory method. In addition, electrostatic potential maps and electron density maps of the dyes were evaluated by AIM (atoms in molecules) analysis. Moreover, the new dyes exhibited potent antibacterial activity and their antibacterial activities (MIC) against Gram-positive and Gram-negative bacterial species were determined.

Keywords: imidazo[1,2-*a*]pyridine, optical properties, density function theory calculations, 3D-electrostatic potential maps, antibacterial activity

Heterocyclic dyes are one of the most important and versatile class of synthetic organic compounds, with an enormous variety of applications. In recent years, heterocyclic dyes have found great success because of their higher tinctorial strength, brighter dyeing and excellent light, washing and sublimation fastness, and chromophoric strength in relation to synthetic organic dyes based uniquely on benzene derivatives.[1] Heterocyclic dyes have wide applications as high-level dying agents in the dyestuff industries.[2,3] The increasing usage of these dyes in the electronics industry, such as colorimetric sensors, nonlinear optical (NLO) devices and liquid crystalline displays (LCDs) have been investigated as has their potential as sensitisers for photodynamic therapy (PDT) that has attracted much attention.[4] Also, they have been evaluated and employed in the new areas of optoelectronic devices,[5] photoconductors,[6] solar-energy utilisation,[7] sensitisers,[8] biomedical probes,[9] photo-catalysts,[10] and so on. Furthermore, heterocyclic dyes have been used extensively in the preparation of disperse dyes with outstanding dischargeability on cellulose acetate.[11]

On the other hand, imidazo[1,2-*a*]pyridines are bicyclic ring systems with multiple applications. They are potent biological agents and possess potent activities such as antiviral,[12] anticancer,[13] anxiolytic,[14] antimalarial,[15] hypnotic,[16] antiprotozoal,[17] and anti-inflammatory[18] agents, which has rendered this ring system an attractive target. Recently, imidazo[1,2-*a*]pyridine moieties became of interest as dyes and fluorescent compounds.[19–21] Furthermore, the analytical properties of some imidazo[1,2-*a*]pyridine dyes show they can be used as an acid-base indicator.[22]

Taking these facts into consideration and in continuation of our previous studies on the synthesis of new heterocyclic dyes,[19–24] in the present study, we have synthesised some new heterocyclic indigo-coloured, purple and orange dyes derived from 3-nitroimidazo[1,2-*a*]pyridine. The key intermediate 2-[3-(hydroxyimino)imidazo[1,2-*a*]pyridin-2(3*H*)-ylidene] malononitrile was obtained *via* the nucleophilic substitution of hydrogen[25] in 3-nitroimidazo[1,2-*a*]pyridine with malononitrile in KOH/MeOH, in high yield. In addition, tautomerism, oxidation, alkylation, optical properties, DFT/TD-DFT calculations, AIM (atoms in molecules) analyses and antibacterial activity of the dyes have also been examined.

Results and discussion

As depicted in Scheme 1, the reaction of 2-aminopyridine with 2-bromo-1,1-dimethoxyethane and then nitration of imidazo[1,2-*a*] pyridine in H_2SO_4 and HNO_3 led to the formation of 3-nitroimidazo[1,2-*a*]pyridine (**1**).[26] When 3-nitroimidazo[1,2-*a*]pyridine **1** and malononitrile **2** were reacted in basic MeOH solution, the new 2-[3-(hydroxyimino) imidazo[1,2-*a*]pyridin-2(3*H*)-ylidene]malononitrile **3** was obtained *via* nucleophilic substitution of hydrogen[25] in excellent yield (Scheme 1). A plausible mechanism to explain the formation of dye **3** is shown in Scheme 1. The initial steps follow those proposed for the condensation of **1** and **2** in basic MeOH solution.[24]

The structure of the new dye **3** was deduced from its spectral and microanalytical data. The presence of one broad exchangeable peak at δ 11.87 (OH) in the ^{1}H NMR spectrum of **3**, weak 2218 cm^{-1} and 2215 cm^{-1} (diastereotopic CN groups) and broad 3455 cm^{-1} (OH) absorption bands in the FTIR spectrum and a molecular ion peak at *m/z* 211 (M^+) confirmed the structure of dye **3**.

The new purple dye **4** was obtained in excellent yield when compound **3** was heated under reflux in EtOAc (Scheme 2). The IR spectrum of **4** showed a stretching vibration band at 1561 cm^{-1} indicative of an N=O group. The ^{1}H NMR spectrum of **4** showed a singlet at δ 5.55 for the methine proton while the ^{13}C NMR spectrum displayed a signal at δ 23.4 confirming the presence of the dicyanomethyl group. The mass spectrum of **4** showed the molecular ion peak at *m/z* 211 (M^+) corresponding to the molecular formula $C_{10}H_5N_5O$.

The new orange dye **5** was obtained from the oxidation of purple dye **4** with 30% H_2O_2 in MeOH in high yield (Scheme 2). The structural assignments of compound **5** were based on the analytical and spectral data. For example, in the IR spectrum of **5**, two strong absorption bands at 1337 and 1543 cm^{-1} are

* Correspondent. E-mail: mehdipordel58@mshdiau.ac.ir

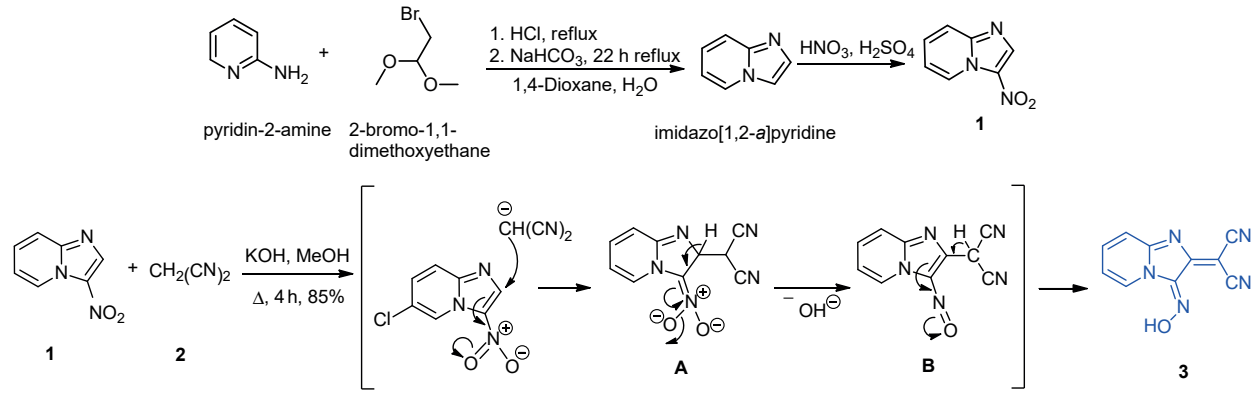

Scheme 1 Synthesis route and reaction mechanism for formation of new indigo-coloured dye **3**.

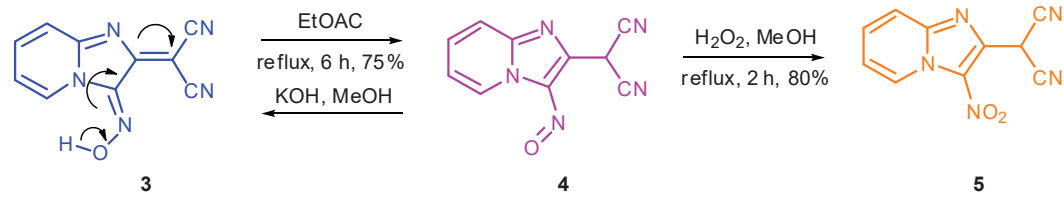

Scheme 2 Synthesis of new purple dye **4** and orange dye **5**.

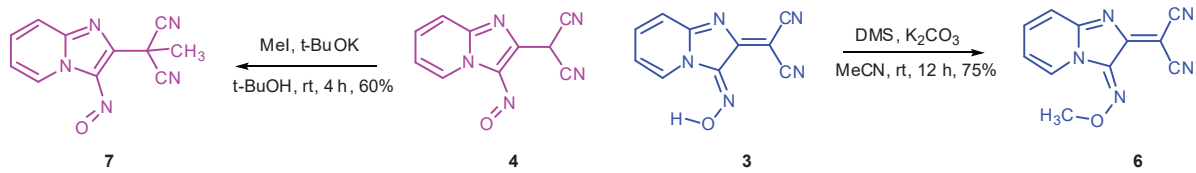

Scheme 3 Methylation of dyes **3** and **4** to new dyes **6** and **7**.

assignable to the nitro group. Furthermore, the mass spectrum of **5** showed the molecular ion peak at *m/z* 227 (M^+) corresponding to the molecular formula $C_{10}H_5N_5O_2$.

The purple solution of dye **4** in KOH/MeOH was smoothly turned to an indigo colour and dye **3** was precipitated after neutralisation of the solution with dilute HCl. It can be concluded that dyes **3** and **4** are not particularly stable and they can be converted into each other under appropriate conditions. However, alkylation of active protons in dyes **3** and **4** prevents tautomerisation of these dyes. Compound **3** was methylated by dimethyl sulfate (DMS) in K_2CO_3 and MeCN to give a new indigo-coloured compound, 2-[3-(methoxyimino) imidazo[1,2-*a*]pyridin-2(3*H*)-ylidene]malononitrile **6** at room temperature (Scheme 3). New purple dye, 2-methyl-2-(3-nitrosoimidazo[1,2-*a*]pyridin-2-yl)malononitrile **7** was also synthesised from the reaction of dye **4** with methyl iodide in *tert*-butanol in the presence of potassium *tert*-butoxide, in high yield (Scheme 3). All the newly synthesised dyes have been characterised by elemental analysis and spectroscopic data. The spectral details of all these are given in the experimental section.

The new dyes **3**–**7** were characterised by their UV-Vis spectra in the region 200–800 nm. Figure 1 shows the visible absorption spectrum of compounds **3**–**7** in dilute (1×10^{-5} M) methanol solution. Characteristics of the absorption spectra for **3**–**7** in methanol are presented in Table 1. Values of the extinction coefficient (ε) were calculated as the slope of the plot of absorbance *vs* concentration. The absorbance intensity and extinction coefficient (ε) in the indigo-coloured dye **3** were the biggest values.

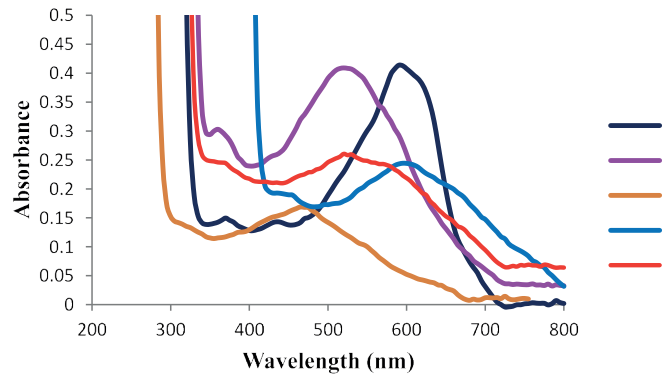

Fig. 1 Visible absorption spectra of compounds **3**–**7** in methanol solution (1×10^{-5} mol L^{-1}).

Table 1 Spectroscopic properties of dyes **3**–**7** in MeOH solvent

Dye	3	4	5	6	7
λ_{max} (nm)[a]	605	525	480	595	520
$\varepsilon \times 10^{-3}$ (M^{-1} cm^{-1})[b]	41.0	40.7	16.8	24.1	25.5

[a]Wavelengths of maximum absorbance (λ_{max}).
[b]Extinction coefficient.

The absorption spectra of dyes **3**–**7** were measured in different solvents. As shown in Table 2, the absorption spectra of **3**–**7** in polar solvents undergo a red shift. Increasing the solvent polarity stabilises the excited state molecule comparative to the ground-state molecule with the observed red shift of the absorption maximum as the experimentally observed result

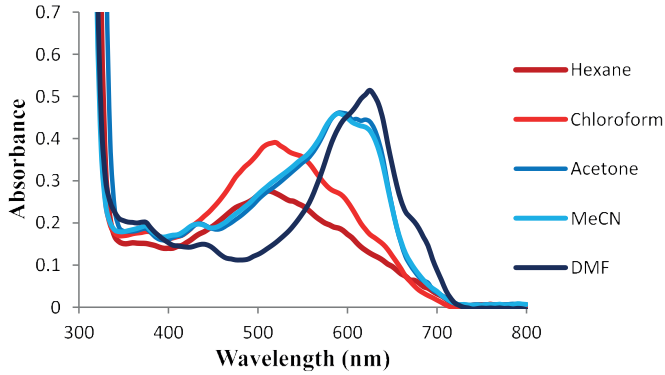

Fig. 2 Visible absorption spectra of compound **3** in different solvents (1×10^{-5} mol L^{-1}).

Table 2 Spectroscopic data for **3–7** at 298 K in dependence of the solvent

Solvent	λ_{abs}/nm (**3**)	λ_{abs}/nm (**4**)	λ_{abs}/nm (**5**)	λ_{abs}/nm (**6**)	λ_{abs}/nm (**7**)
n-Hexane	505	500	455	505	495
Chloroform	520	505	465	525	505
Acetone	595	515	480	595	515
MeCN	595	520	480	595	520
DMF	625	530	485	620	525

(Tables 2). For example, in the absorption spectra of indigo-coloured **3**, λ_{abs} shifts from 505 to 625 nm, as the solvent changes from *n*-hexane to DMF (Fig. 2 and Table 2).

The colour intensity of dyes **3–7** indicates efficient intramolecular charge transfer (ICT) states[23] from the donor site (endocyclic N-4 in dyes **3–7** or OH group in dyes **3** and **6**) to the acceptor moiety (CN in dyes **3** and **6** or N=O group in dyes **4**, **5** and **7**). To gain a deeper insight into the optical properties and the UV-Vis absorption spectra of the dyes, we performed DFT and TD-DFT (time-dependent density functional theory) calculations at the B3LYP/6-311++G(d,p) level and obtained the optimised geometries, HOMO and LUMO frontier orbitals and electronic spectra of dyes **3–5**.

The optimised geometries of the compounds **3–5** are shown in Fig. 3. In the optimised geometry of the dye **3**, imidazo[1,2-*a*] pyridine ring and cyano groups are essentially planar and the C=C bond lengths (1.38–1.44 Å) of the aromatic rings are in the expected range[27] (Tables S1–S3; see ESI).

The energy difference between the HOMO and LUMO frontier orbitals is one of the important characteristics of molecules, which has a determining role in such cases as electrical properties, electronic spectra and photochemical reactions. The HOMO and LUMO maps of **3–5** are shown in Fig. 4. Separation energies between the HOMO and LUMO ($\Delta\varepsilon = \varepsilon_{LUMO} - \varepsilon_{HOMO}$) in dyes **3–5** are 2.78, 3.35 and 3.97 eV, respectively. It can be seen from Fig. 4 that dye **3** has more π-system overlap in its HOMO and LUMO frontier orbitals which led to the lower separation energy between the HOMO and LUMO compared to dyes **4** and **5.** In the ESI (Scheme S1), neutral and some charge-separated mesomeric structures of dyes **3–5** are presented.

Calculated electronic absorption spectra were also obtained by time-dependent density functional theory (TD-DFT) method. The TD-DFT electronic spectra calculations on **3** show two electronic transition bands. There is a relatively sharp peak at 316 nm (oscillator strength: 0.0003), which can be attributed to π–π* transitions (donor endocyclic N-4 to the acceptor CN group), and a relatively broad band in the range of 400 to 700 nm with an oscillator strength of 0.2899, which can be linked to n–π* transitions from the donor OH group to the acceptor CN group, compared with the experimental values of 500–700 nm. The TD-DFT electronic spectra calculations of **4** reveal a relatively sharp peak in the range of 450 to 650 nm which corresponds to the experimental data (400–600 nm) with oscillator strength of 0.2414. These bands can be linked to π–π* transitions from the donor endocyclic N-4 to the acceptor N=O group. Also, the TD-DFT electronic spectra calculations on dye **5** show that there is a relatively sharp peak at 447 nm (oscillator strength: 0.2836), which can be attributed to π–π* transitions from donor endocyclic N-4 to the acceptor NO_2 group. This electronic transition band can be compared with the experimental values of 480 nm.

The calculated electronic absorption spectra of compounds **3–5** are shown in the ESI (Fig. S1–S3).

AIM analysis

The electrostatic potential map, $V_S(r)$,[28] of three dye's structures are shown in Fig. 5. As is clear from the 3D-electrostatic potential maps, dye **3** due to a strong resonance has a greater charge distribution throughout the structure, but as can be seen from the electrostatic potential maps of structures **4** and **5**, there is noticeable charge separation.

In Fig. 5, the negative potential region $V_S(r)$ is located at the outermost part of CN and shown in red.

On the other hand, according to the 3D-electron density map (Fig. 6) is well defined that the structure **3** due to its planar structure has a good chance to resonance than other structures having nonplanar structure, which is principally associated with the π-electronic structure; this advantage has led to much denser electron density on CN groups.

The antibacterial activity of compounds **3–7** was tested against standard strains of two Gram-negative bacteria (*Salmonella typhimurium* ATCC 14028 and *Escherichia coli* ATCC 10538) and two Gram-positive (*Staphylococcus aureus* ATCC 29213 and *Bacillus subtilis* ATCC 6633) species (Table 3), using the broth microdilution method as previously described.[29] Amoxicillin and ciprofloxacin were used as reference compounds in the study on the antibacterial activity.

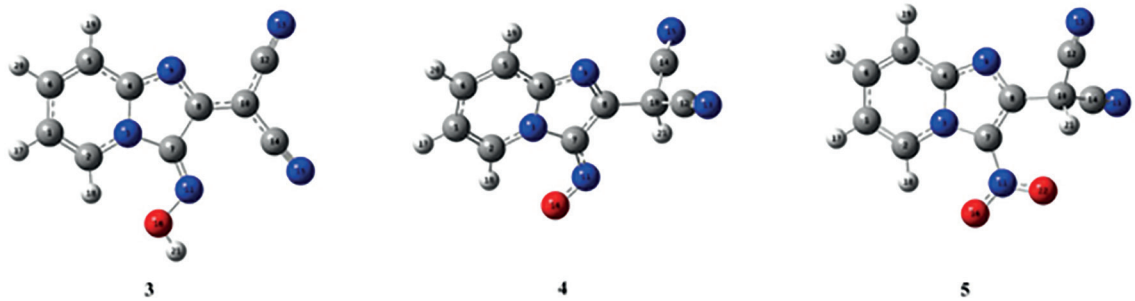

Fig. 3 Optimised geometries of the new dyes **3–5**.

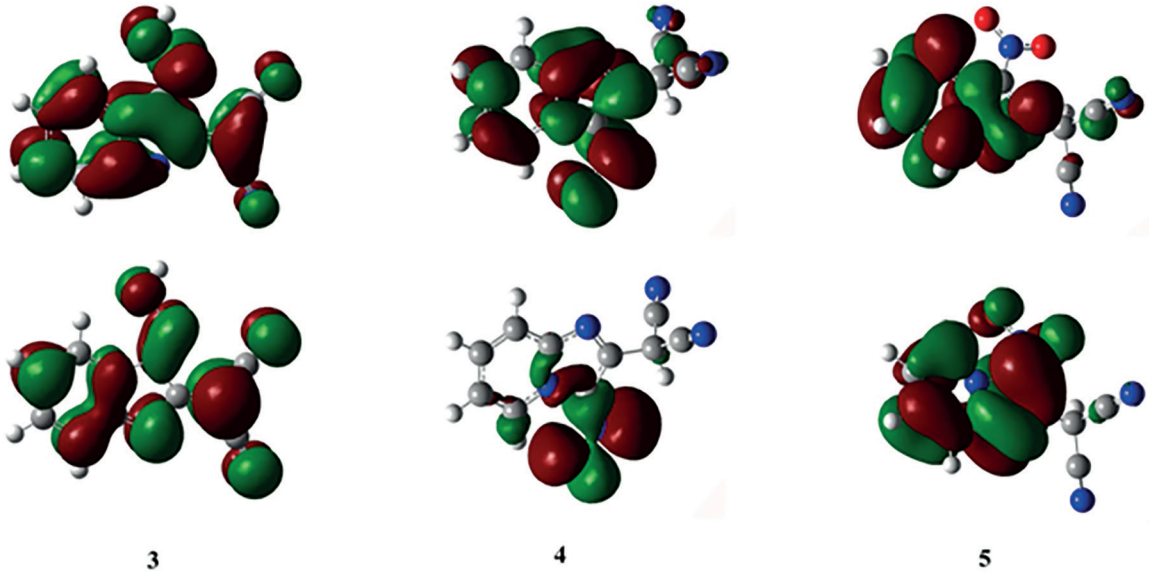

Fig. 4 The HOMO (lower) and LUMO (upper) frontier orbitals of the dyes **3–5**.

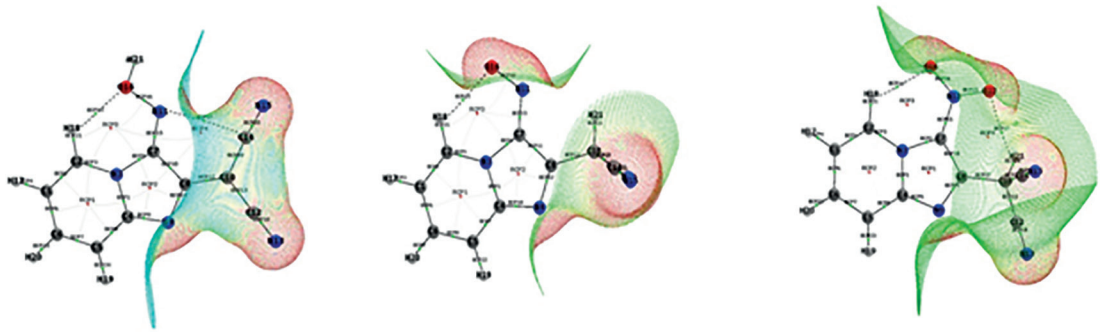

Fig. 5 The 3D-electrostatic potential maps of dyes **3–5**.

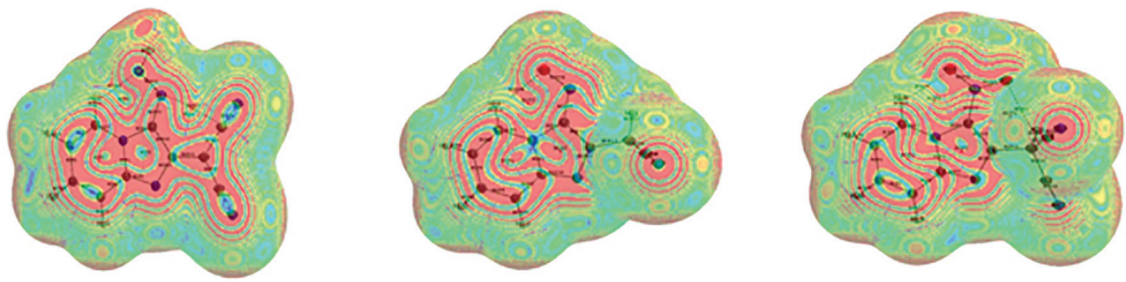

Fig. 6 The 3D-electron density maps of dyes **3–5**.

The lowest concentration of the antibacterial agent that prevents growth of the test organism, as detected by lack of visual turbidity (matching the negative growth control), is assigned the minimum inhibitory concentration (MIC). Experimental details of the tests can be found in our earlier studies.[20,30,31]

As demonstrated in Table 3, compounds **3–7** are effective against both Gram-positive and Gram-negative bacteria. The test results revealed that compounds **4** and **7** (nitroso compounds) show the greater inhibitory effects against *Escherichia coli* ATCC 10538, *Salmonella typhimurium* ATCC 14028, *Staphylococcus aureus* ATCC 29213, and *Bacillus subtilis* ATCC 6633 species than the other compounds. Moreover, as the data in Table 3 reveals, the antibacterial activity of the alkylated compounds **6** and **7** is higher compared to that of compounds **3** and **4** respectively. Gratifyingly, compound **7** shows higher antibacterial activity against the *Salmonella typhimurium* ATCC 14028, *Staphylococcus aureus* ATCC 29213 and *Escherichia coli* ATCC 10538 species compared to the well-known antibacterial agents ciprofloxacin and amoxicillin (Table 3).

Conclusion

In conclusion, we have synthesised some new donor-acceptor indigo-coloured, purple and orange heterocyclic dyes from imidazo[1,2-*a*]pyridine. The interesting optical properties of the dyes were examined and the solvent effects on the absorption spectra of the dyes were studied. DFT and TD-DFT calculations of the dyes **3–5** were performed to gain a deeper insight into the charge transfer properties, optimised geometries, HOMO and LUMO frontier orbitals and electronic spectra by using the

Table 3 Inhibitory activity (MIC, μg mL^{-1}) of references and compounds **3–7** against bacteria

Compound	*Staphylococcus aureus* (ATCC 29213)	*Bacillus subtilis* (ATCC 6633)	*Escherichia coli* (ATCC10538)	*Salmonella typhimurium* (ATCC14028)
3	75	25	50	150
4	25	1	1	75
5	50	5	15	150
6	75	15	15	50
7	5	0.5	0.5	50
Ciprofloxacin	16	0.05	1	>128
Amoxicillin	25	0.06	150	>128

B3LYP hybrid functional and the 6-311++G(d,p) basis set. The results showed that the imidazo[1,2-*a*]pyridine ring and cyano groups in dye **3** are essentially planar and the separation energies between the HOMO and LUMO in dyes **3**–**5** were 2.78, 3.35 and 3.97 eV, respectively. Also, electronic spectra of dyes **3**–**5** were in relatively good agreement with visible absorption spectra. In addition, AIM analysis was conducted to investigate the 3D-electrostatic potential maps and 3D-electron density maps in these dyes. The results show that concentration of electron density through the C–N bond in the cyano fragment of three dyes is different, and dye **3** has a greater charge distribution throughout the structure due to a strong resonance. Comparing the quantum-chemical investigations with the experimental results reveals that they are in good agreement and DFT and TD-DFT calculations and AIM analysis can prove the higher maximum absorption wavelength in dye **3** compared to **4** and **5**. Moreover, results from the antimicrobial screening tests show the synthesised compounds are effective against standard strains of Gram-positive and Gram-negative growth inhibitors. This property, together with optical properties, can offer an excellent opportunity for the study of physiological functions of bacteria such as at single-cell level.[32]

Further investigation into the scope and application of these new dyes is in progress and will be reported soon.

Experimental

Methanol, acetone, acetonitrile, chloroform, *n*-hexane, *N,N*-dimethylformamide (DMF), methyl iodide, dimethyl sulfate (DMS), potassium *tert*-butoxide, *tert*-butanol, 2-aminopyridine, 2-bromo-1,1-dimethoxyethane and malononitrile were purchased from Merck. Amoxicillin, ciprofloxacin and potassium hydroxide was purchased from Sigma-Aldrich. The microorganisms *Escherichia coli* ATCC 10538, *Salmonella typhimurium* ATCC 14028, *Staphylococcus aureus* ATCC 29213 and *Bacillus subtilis* ATCC 6633 were purchased from Pasteur Institute of Iran. All solvents were dried according to standard procedures. Compound **1** was synthesised as described in the literature.[26]

Absorption spectra were recorded on a Varian Cary 50-bio UV-Vis spectrophotometer. UV-Vis scans were recorded from 200 to 800 nm. Melting points were measured on an Electrothermal type-9100 melting-point apparatus. The IR (as KBr discs) spectra were obtained on a Tensor 27 spectrometer and only noteworthy absorptions are listed. The ^{13}C NMR (100 MHz) and the ^{1}H NMR (400 MHz) spectra were recorded on a Bruker Avance DRX-400 Fourier-transform spectrometer for DMSO-d_6 and $CDCl_3$ solutions. Chemical shifts are reported in parts per million downfield from TMS as the internal standard; coupling constants *J* are given in hertz. The mass spectra were recorded on a Varian Mat, CH-7 at 70 eV. Elemental analysis was performed on a Thermo Finnigan Flash EA microanalyser. All measurements were carried out at room temperature.

DFT calculations have been performed with the Gaussian 98 software package[33] by using the B3LYP hybrid functional[34] and the 6-311++G (d,p) basis set. Firstly, geometry of the compounds **3**–**5** was fully optimised in the MeOH solution.

Here, one of the self-consistent reaction field methods, the sophisticated Polarised Continuum Model (PCM)[35] has been used for investigation of the solvent effects. The PCM calculations have been performed in the MeOH solution and the zero-point corrections were considered to obtain energies. Based on the optimised geometries and TD-DFT[36–38] methods, the electronic spectra of the compounds **3**–**5** were predicted.

Synthesis of **3** *from* **1** *and* **2**

3-Nitroimidazo[1,2-*a*]pyridine (**1**) (3.26 g, 20 mmol) and malononitrile (**2**) (1.98 g, 30 mmol) were added with stirring to a solution of KOH (20 g, 357 mmol) in methanol (70 mL). The mixture was refluxed with stirring for 4 h, and then poured into water. After neutralisation with dilute HCl solution, the precipitate was collected by filtration, washed with water and then air dried to give crude **3**. More purification was achieved by crystallisation from acetone-H_2O (1:1).

*2-[3-(Hydroxyimino)imidazo[1,2-*a*]pyridin-2(3*H*)-ylidene] malononitrile* (**3**) was obtained as a dark indigo-coloured powder (acetone-H_2O; 1:1), yield 85%, m.p. >300 °C; IR (KBr disk): ν_{max}/cm^{-1} 3455 (OH), 2218 and 2215 (diastereotopic CN groups); ^{1}H NMR (DMSO-d_6): δ 7.69 (1H, d, *J* = 5.5 Hz, ArH), 7.75 (1H, d, *J* = 7.1 Hz, ArH), 7.91–8.05 (2H, m, ArH), 11.87 (1H, br s, OH); ^{13}C NMR ($CDCl_3$): δ 85.7, 112.5, 112.7, 114.6, 126.0, 135.6, 137.5, 151.3, 151.7, 168.5; MS (*m/z*) 211 (M$^+$). Anal. calcd for $C_{10}H_5N_5O$ (211.2): C, 56.87; H, 2.39; N, 33.16; found: C, 56.71; H, 2.36; N, 32.97%.

Synthesis of **4** *from* **3**

The indigo-coloured solution of dye **3** (1.05 g, 5 mmol) in EtOAc (50 mL) was heated for 6 h under reflux. After concentration of the purple solution at reduced pressure, the precipitate was recrystallised from MeOH to give pure dye **4**.

*2-(3-Nitrosoimidazo[1,2-*a*]pyridin-2-yl)malononitrile* (**4**) was obtained as dark purple powder (MeOH), yield 75%, m.p. >300 °C; IR (KBr disk): ν_{max}/cm^{-1} 2204 (CN), 1561 (N=O); ^{1}H NMR (DMSO-d_6): δ 5.55 (1H, s, benzylic H), 6.67 (1H, td, J_1 = 7.1 Hz, J_2 = 1.2 Hz, ArH), 6.78 (1H, td, J_1 = 5.5 Hz, J_2 = 1.5 Hz, ArH), 7.53 (1H, d, *J* = 5.5 Hz, ArH), 7.67 (1H, d, *J* = 7.1 Hz, ArH); ^{13}C NMR ($CDCl_3$): δ 23.4, 110.7, 114.1, 114.8, 126.8, 127.4, 127.8, 142.6, 147.6; MS (*m/z*) 211 (M$^+$). Anal. calcd for $C_{10}H_5N_5O$ (211.2): C, 56.87; H, 2.39; N, 33.16; found: C, 56.67; H, 2.34; N, 32.89%.

Synthesis of **5** *from* **4**

H_2O_2 (0.55 mL, 30%, 2 mmol) was added to a stirred solution of dye **4** (0.2 g, 1 mmol) in MeOH (5.0 mL) at 60 °C. After the 2 h, the orange solution was diluted with H_2O (50 mL), chilled and filtered, and then the solid was washed with H_2O and air dried to give crude **5**. Dye **5** was recrystallised from MeOH.

*2-(3-Nitroimidazo[1,2-*a*]pyridin-2-yl)malononitrile* (**5**) was obtained as orange needles (MeOH), yield 80%, m.p. 253–255 °C; IR (KBr disk): ν_{max}/cm^{-1} 2245 (CN), 1337, 1543 (NO_2). ^{1}H NMR (DMSO-d_6): δ 5.63 (1H, s, benzylic H), 6.71 (1H, td, J_1 = 7.1 Hz, J_2 = 1.2 Hz, ArH), 6.75 (1H, td, J_1 = 5.5 Hz, J_2 = 1.5 Hz, ArH), 7.69 (1H, d, *J* = 5.5 Hz, ArH), 7.81 (1H, d, *J* = 7.1 Hz, ArH); ^{13}C NMR ($CDCl_3$): δ 24.1, 111.1, 114.4, 114.6, 126.8, 127.2, 140.1, 142.9, 158.1; MS (*m/z*) 227 (M$^+$). Anal. calcd for $C_{10}H_5N_5O_2$ (227.2): C, 52.87; H, 2.22; N, 30.83; found: C, 52.69; H, 2.19; N, 30.75%.

Synthesis of **6** *from* **3**

Dimethyl sulfate (DMS) (0.9 g, 7 mmol) and K_2CO_3 (5.5 g, 40 mmol) were added to an indigo-coloured solution of compound **3** (1.02 g,

5 mmol) in acetonitrile (40 mL). The mixture was stirred for 12 h at room temperature and then poured into water. The product was extracted with CH_2Cl_2 (2 × 50 mL). The extract was dried ($MgSO_4$), treated with charcoal and evaporated to give crude **6**. Further purification was achieved by recrystallisation from acetone.

*2-[3-(Methoxyimino)imidazo[1,2-*a*]pyridin-2(3*H*)-ylidene] malononitrile* (**6**) was obtained as indigo-coloured needles (acetone), yield 72%, m.p. 195–197 °C; IR (KBr disk): ν_{max}/cm^{-1} 2223 and 2219 (diastereotopic CN groups); ^{1}H NMR ($CDCl_3$): δ 4.21 (s, 3H, OCH_3), 7.71 (1H, d, *J* = 5.5 Hz, ArH), 7.74 (1H, d, *J* = 7.1 Hz, ArH), 7.95–8.07 (2H, m, ArH); ^{13}C NMR ($CDCl_3$): δ 63.6, 84.6, 112.7, 113.4, 114.6, 125.3, 136.1, 137.3, 151.2, 151.8, 168.9; MS (*m/z*) 225 (M^+). Anal. calcd for $C_{11}H_7N_5O$ (225.2): C, 58.67; H, 3.13; N, 31.10; found: C, 58.49; H, 3.12; N, 30.88%.

Synthesis of **7** *from* **4**

Methyl iodide (1.4 g, 10 mmol) and potassium *tert*-butoxide (1.12 g, 10 mmol) were added to a solution of compound **4** (2.76 g, 10 mmol) in *tert*-butanol (50 mL). After the mixture was stirred for 4 h at room temperature, it was concentrated at reduced pressure and then water (50 mL) was added to the mixture. The product was extracted with CH_2Cl_2 (2 × 40 mL). The extract was dried ($MgSO_4$), treated with charcoal and evaporated to give crude **7.** Further purification was performed by recrystallisation from *n*-hexane-EtOAc (1:1).

*2-Methyl-2-(3-nitrosoimidazo[1,2-*a*]pyridin-2-yl)malononitrile* (**7**) was obtained as a purple powder (acetone), yield 65%, m.p. 169–172 °C; IR (KBr disk): ν_{max}/cm^{-1} 2204 (CN), 1535 (N=O); ^{1}H NMR (DMSO-d_6): δ 2.33 (3H, s, CH_3), 6.72 (1H, td, J_1 = 7.2 Hz, J_2 = 1.2 Hz, ArH), 6.76 (1H, td, J_1 = 5.6 Hz, J_2 = 1.5 Hz, ArH), 7.61 (1H, d, *J* = 5.6 Hz, ArH), 7.64 (1H, d, *J* = 7.2 Hz, ArH); ^{13}C NMR ($CDCl_3$): δ 19.5, 22.9, 110.5, 112.5, 115.3, 126.7, 127.5, 128.3, 142.5, 147.1; MS (*m/z*) 225 (M^+). Anal. calcd for $C_{11}H_7N_5O$ (225.2): C, 58.67; H, 3.13; N, 31.10; found: C, 58.41; H, 3.10; N, 30.95%.

Acknowledgments

We would like to express our sincere gratitude to Research Office, Mashhad Branch, Islamic Azad University, Mashhad-Iran, for financial support of this work. We also acknowledge Maryam Jajarmi (Khorasan Razavi Rural Water and Wastewater Co.) for her assistance with antibacterial studies.

Electronic supplementary information

The ESI (bond lengths and angles, mesomeric structures and calculated UV-Vis spectra of compounds **3–5**) is available through stl.publisher.ingentaconnect.com/content/stl/jcr/supp-data.

Received 30 August 2016; accepted 20 January 2017
Paper 1604295 DOI: 10.3184/174751917X14873588907684
Published online: 3 March 2017

References

1 H. Yousefi, A.Yahyazadeh, M.R. Yazdanbakhsh, M. Rassa and E.O. Moradi-e-Rufchahi, *J. Mol. Struct*., 2012, **1015**, 27.
2 H.S. Bhatti and S. Seshadri, *Color. Technol*., 2004, **120**, 151.
3 A.H. Shridhar, J. Keshavayya and J. Hoskeri, *Int. J. Pharm. Pharm. Sci*., 2002, **4**, 386.
4 H. Faustino, R.M. El-Shishtawy, L.V. Reis, P.F. Santos and P. Almeida, *Tetrahedron Lett*., 2008, **49**, 6907.
5 K. Kalyanasundaram and M. Grätzel, *Coord. Chem. Rev*., 1998, **177**, 347.
6 S. Aihara, Y. Hirano, T. Tajima, *et al*., *Appl. Phys. Lett*., 2003, **82**, 511.
7 A.S. Polo, M.K. Itokazu and N.Y.M. Iha, *Coord. Chem. Rev*., 2004, **248**, 1343.
8 J. Shi, Z. Chai, J. Su, *et al*., *Dyes Pigm*., 2013, **98**, 405.
9 E. Te Velde, T. Veerman, V. Subramaniam and T. Ruers, *Eur. J. Surg. Oncol*., 2010, **36**, 6.
10 C.-L. Hsueh, Y.-W. Lu, C.-C. Hung, Y.-H. Huang and C.-Y. Chen, *Dyes Pigm*., 2007, **75**, 130.
11 H.R. Maradiya, *J. Saudi Chem. Soc*., 2010, **14**, 77.
12 K.S. Gudmundsson and B.A. Johns, *Org. Lett*., 2003, **5**, 1369.
13 Z. Wu, M.E. Fraley, M.T. Bilodeau, *et al*., *Bioorg. Med. Chem. Lett*., 2004, **14**, 909.
14 A. Geronikaki, E. Babaev, J. Dearden, *et al*., *Bioorg. Med. Chem.,* 2004, **12**, 6559.
15 P.C. Lima, M.A. Avery, B.L. Tekwani, H. de M Alves, E.J. Barreiro and C.A. Fraga, *Farmaco*, 2002, **57**, 825.
16 G. Trapani, M. Franco, L. Ricciardi, *et al*., *J. Med. Chem*., 1997, **40**, 3109.
17 M.A. Ismail, R. Brun, T. Wenzler, F.A. Tanious, W.D. Wilson and D.W. Boykin, *J. Med. Chem*., 2004, **47**, 3658.
18 Y. Abe, H. Kayakiri, S. Satoh, *et al*., *J. Med. Chem*., 1998, **41**, 4053.
19 M. Rahimizadeh, M. Pordel, M. Bakavoli and H. Eshghi, *Dyes Pigm*., 2010, **86**, 266.
20 M.M.F. Baf, M. Pordel and L.R. Daghigh, *Tetrahedron Lett*., 2014, **55**, 6925.
21 M. Rahimizadeh, M. Pordel, M. Ranaei and M. Bakavoli, *J. Heterocycl. Chem*., 2012, **49**, 208.
22 S. Razmara, M. Pordel and M. Ebrahimi, *Chem. Heterocycl. Compd*., 2015, **51**, 713.
23 S. Poorhaji, M. Pordel and S. Ramezani, *J. Mol. Struct*., 2016, **1119**, 151.
24 M. Pordel, S.A. Beyramabadi and A. Mohammadinejad, *Dyes Pigm*., 2014, **102**, 46.
25 M. Mąkosza and K. Wojciechowski, *Chem. Rev*., 2004, **104**, 2631.
26 26 J.P. Paolini and R.K. Robins, *J. Org. Chem*., 1965, **30**, 4085.
27 27 H. Dal, Y. Süzen and E. Şahin, *Spectrochim. Acta Part A*., 2007, **67**, 808.
28 28 C.F. Matta, A.A. Arabi and D.F. Weaver, *Eur. J. Med. Chem*., 2010, **45**, 1868.
29 S.M. Finegold and L. Garrod, *Bailey and Scott's diagnostic microbiology*, 8th edn. C.V. Mosby, Toronto, 1995, chap. 13, pp. 171.
30 M. Pordel, S. Ramezani, M. Jajarmi and M. Sokhanvar, *Russ. J. Bioorg. Chem*., 2016, **42**, 106.
31 M. Pordel, A. Abdollahi and B. Razavi, *Russ. J. Bioorg. Chem*., 2013, **39**, 240.
32 F. Joux and P. Lebaron, *Microbes Infect*., 2000, **2**, 1523.
33 M.J. Frisch, G.W. Trucks, H.B. Schlegel, *et al*., *Gaussian 98, Revision A.7*, Gaussian, Inc. Pittsburgh PA, 1998.
34 C. Lee, W. Yang and R.G. Parr, *Phys. Rev.* B, 1988, **37**, 785.
35 R. Cammi and J. Tomasi, *J. Comput. Chem*., 1995, **16**, 1449.
36 D. Bauer and F. Ceccherini, *Opt. Express*, 2001, **8**, 377.
37 M. Petersilka, U. Gossmann and E. Gross, *Phy. Rev. Lett*., 1996, **76**, 1212.
38 R. Bauernschmitt and R. Ahlrichs, *Chem. Phys. Lett*., 1996, **256**, 454.